*Electronic Supplementary Information (ESI)*

# High-index facet engineering of PtCu cocatalyst for superior photocatalytic reduction of $CO_2$ to $CH_4$

Qingqing Lang,‡[a] Yanju Yang,‡[a] Yuzhen Zhu,[a] Wenli Hu,[a] Wenya Jiang,[b] Shuxian Zhong,[a] Peijun Gong,[a] Botao Teng,*[a] Leihong Zhao*[a] and Song Bai*[a,b]

[a] Key Laboratory of the Ministry of Education for Advanced Catalysis Materials，College of Chemistry and Life Sciences, Zhejiang Normal University, Jinhua, Zhejiang, 321004, P. R. China.
[b] School of Chemistry and Materials Science, University of Science and Technology of China, Hefei, Anhui 230026, P. R. China.

*Email: songbai@zjnu.edu.cn

*Email: tbt@zjnu.edu.cn

*Email: zhaoleihong@163.com

‡The first two authors contributed equally to this work.

**Experimental**

**Chemicals.**   Potassium tetrachloroplatinate(I) ($K_2PtCl_4$, Aldrich, 520853), Polyvinylpyrrolidone (PVP, M.W.≈29000, Aldrich, 234257), Chloroplatinic acid hexahydrate ($H_2PtCl_6 \cdot 6H_2O$, Aldrich, C120776), Trioctylphosphine oxide (TOPO, Aldrich, 223301).   All other chemicals were of analytical grade and purchased from Sinopharm Chemical Reagent Co., Ltd.   The water used in all experiments was de-ionized.   All chemicals were used as received without further purification.

**Synthesis of $C_3N_4$-Pt nanocubes.**   In a typical synthesis of $C_3N_4$-Pt nanocubes ($C_3N_4$-Pt NCs), g-$C_3N_4$ powder was dispersed in DMF to form a 5-mg/mL $C_3N_4$ nanosheets suspension with probe sonication (Scientz-IID, China) for 1 h.   Then $H_2PtCl_6 \cdot 6H_2O$ (30 mg/mL, 0.5 mL in N,N-dimethylformamide (DMF)), PVP (K30, 200.0 mg), and 0.1-mL methylamine solution (30%) were mixed in 10-mL DMF dispersion of $C_3N_4$.   The resulted mixture was transferred to a Teflon-lined stainless steel autoclave with capacity of 20 mL and heated at 200 °C for 10.5 h. After the autoclave had cooled down to room temperature, the resultant product was separated by centrifugation, and washed with water and ethanol for several times.   The final product was then dried at 45 °C for 12 h.

**Synthesis of $C_3N_4$-Cu nanocubes.**   In a typical synthesis of $C_3N_4$-Cu nanocubes ($C_3N_4$-Cu NCs), Cu nanocubes were firstly synthesized through a modified method according to the previous literature.[S1]   Typcially, CuBr (0.6 mmol) and TOPO (1.5 mmol) were dissolved into 15 mL of oleylamine under magnetic stirring at 80 °C for 15 min.   Then the temperature was raised to 210 °C quickly, and the reaction was allowed to proceed for 1 h.   The resultant product was separated by centrifugation, and washed with a mixed solution of hexane and acetone for several times, and redispersed in hexane.   Then $C_3N_4$-Cu NCs was obtained by directly depositing Cu nanocubes on $C_3N_4$ nanosheets.   In brief, 10 mg of $C_3N_4$ were dispersed in 5 mL ethanol by sonication. Subsequently, 90 μL hexane suspension (10 mg mL$^{-1}$) of Cu nanocubes was added into the dispersion, which was further sonicated for 10 min.   The as-obtained mixture was kept static for precipitation, centrifuged, and washed with water for several times, then dried at 60 °C in vacuum, and further annealed at 100 °C for 2 h to increase the contact between Cu nanocubes and $C_3N_4$ nanosheets.

**Sample characterizations.** X-ray powder diffraction (XRD) patterns were recorded by using a Philips X'Pert Pro Super X-ray diffractometer with Cu-Kα radiation (λ = 1.54178 Å). X-ray photoelectron spectra (XPS) were collected on an ESCALab 250 X-ray photoelectron spectrometer, using nonmonochromatized Al-Kα X-ray as the excitation source. Transmission electron microscopy (TEM), high-resolution TEM (HRTEM), scanning TEM (STEM) images and energy-dispersive spectroscopy (EDS) mapping profiles were taken on a JEOL JEM-2100F field-emission high-resolution transmission electron microscope operated at 200 kV. The concentrations of metal elements were measured as follows: the samples were dissolved with a mixture of HCl and $HNO_3$ (3:1, volume ratio) which was then diluted with 1% $HNO_3$. The concentrations of metal ions were then measured with a Thermo Scientific PlasmaQuad 3 inductively-coupled plasma mass spectrometry (ICP-MS). The loading amounts of PtCu related to the $C_3N_4$ nanosheets were determined by sample weighing prior to the dissolution of Pt and Cu for the ICP-MS measurements. UV-vis-NIR diffuse reflectance data were recorded in the spectral region of 200-800 nm with a Shimadzu SolidSpec-3700 spectrophotometer. Photoluminescence (PL) spectra were recorded on a HITACHI F-7000 Spectrofluorometer with the excitation wavelength of 390 nm. The Fourier transform infrared (FTIR) measurements were carried out on a Nicolet 8700 FTIR spectrometer in a KBr pellet, scanning from 4000 to 500 $cm^{-1}$.
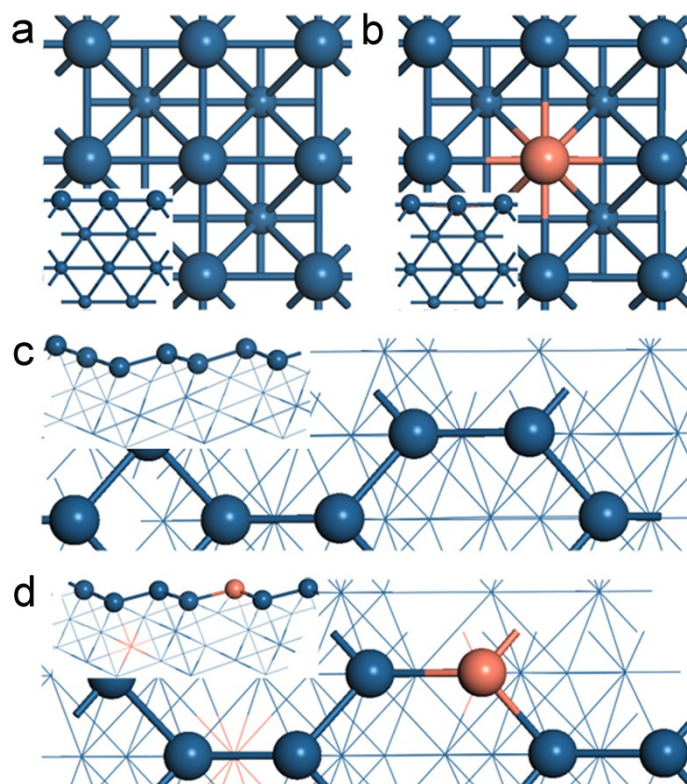
**Fig. S1** Models for (a) Pt(100), (b) PtCu(100), (c) Pt(730) and (d) PtCu(730) (dark blue ball for Pt atom; brown ball for Cu atom).
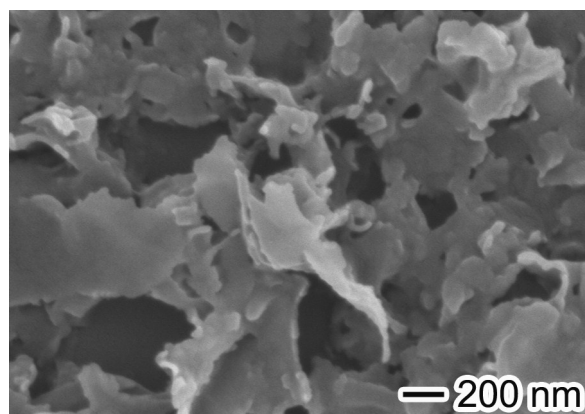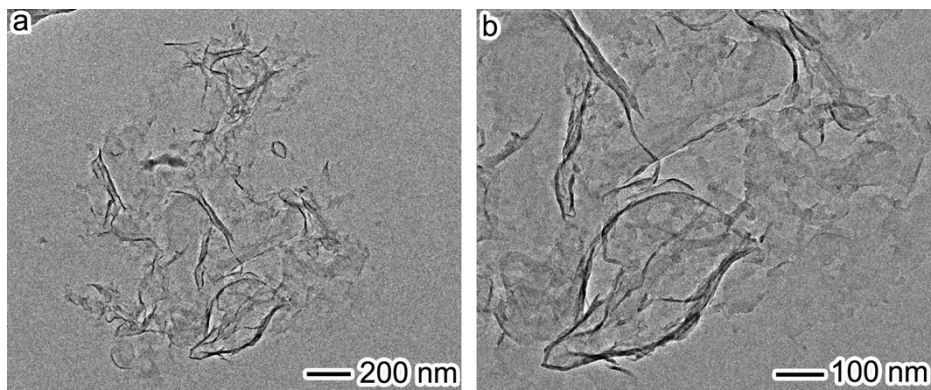
**Fig. S2** SEM image of bulk $C_3N_4$.

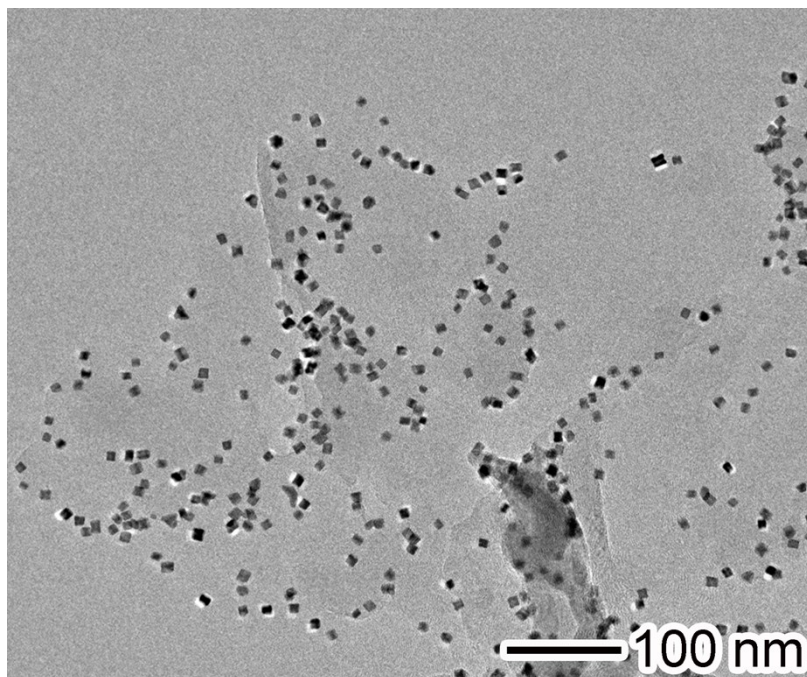**Fig. S3** TEM images of exfoliated $C_3N_4$ nanosheets.

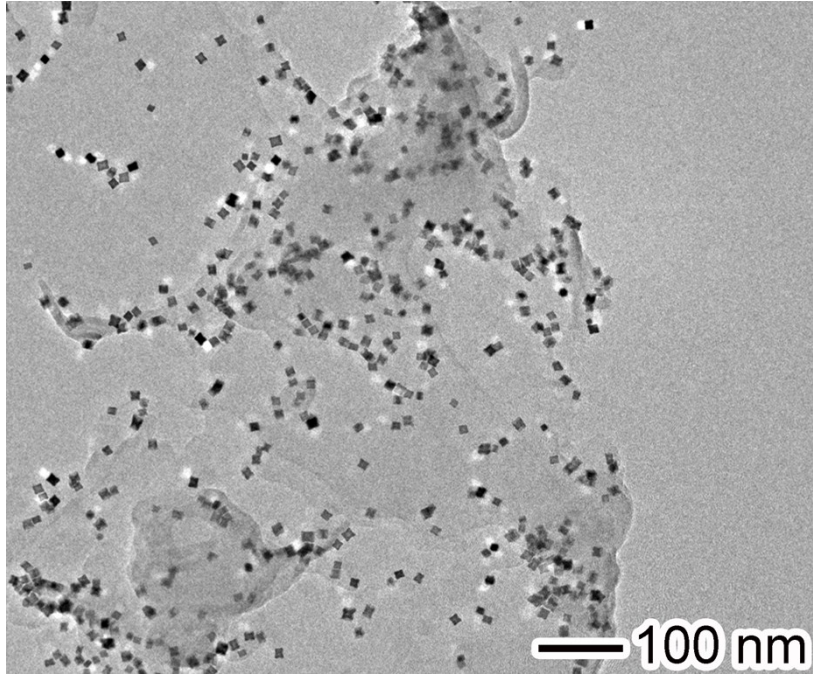**Fig. S4** Low-magnification TEM image of $C_3N_4$-PtCu NCs.

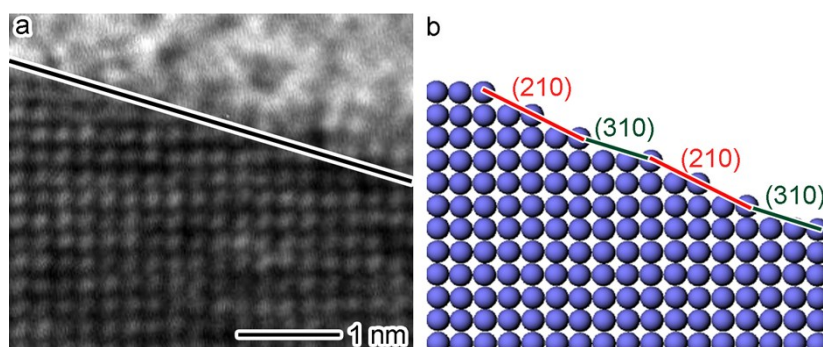**Fig. S5** Low-magnification TEM image of C$_3$N$_4$-PtCu CNCs.

**Fig. S6** (a) HRTEM images of PtCu concave nanocubes on $C_3N_4$ nanosheets; (b) atomic model corresponding to the HRTEM image.
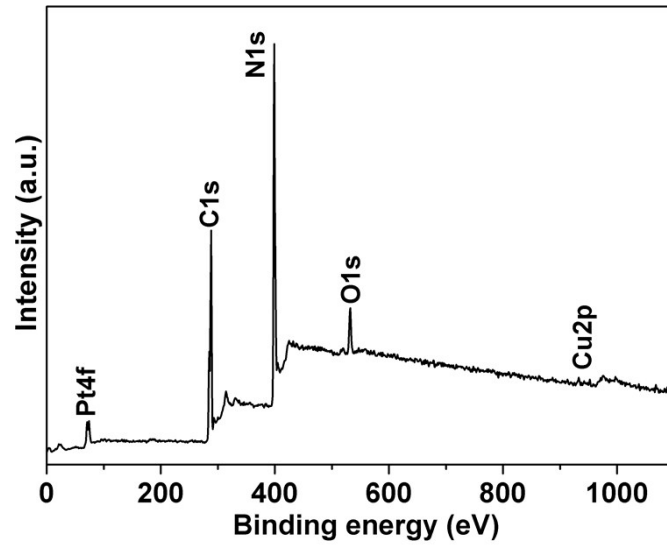
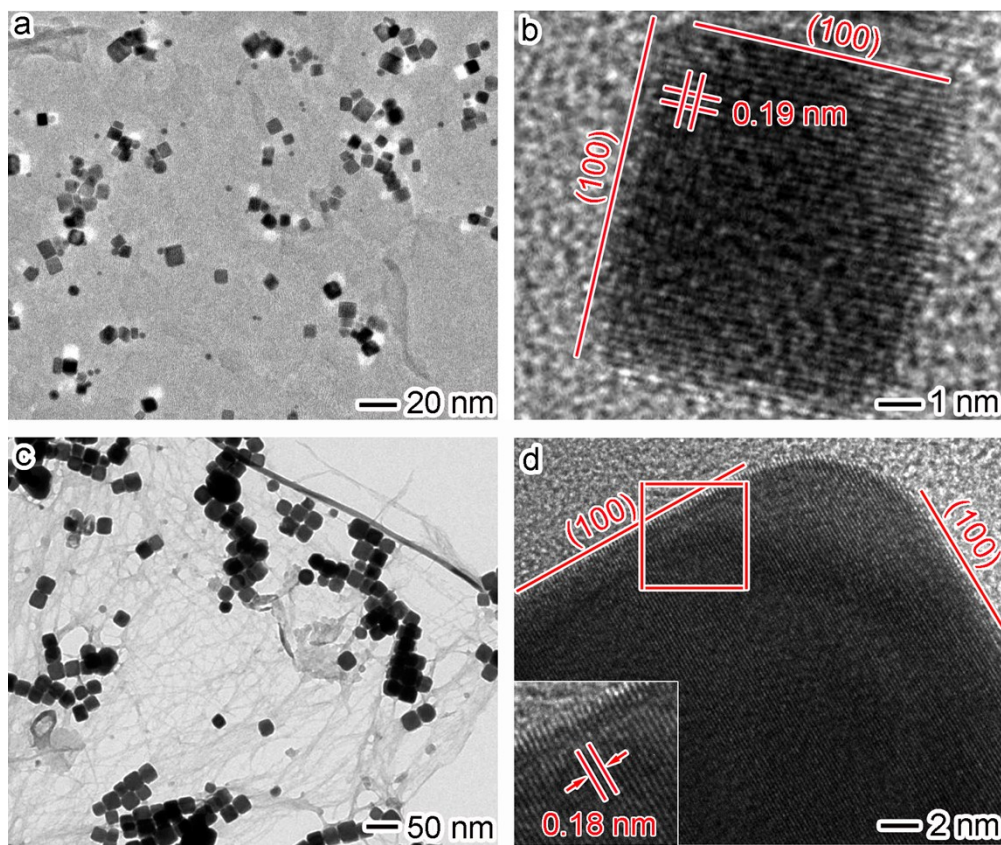**Fig. S7** XPS spectra of $C_3N_4$-PtCu CNCs hybrid structure.

**Fig. S8** TEM and HRTEM images of (a,b) $C_3N_4$-Pt NCs and (c,d) $C_3N_4$-Cu NCs hybrid structures.
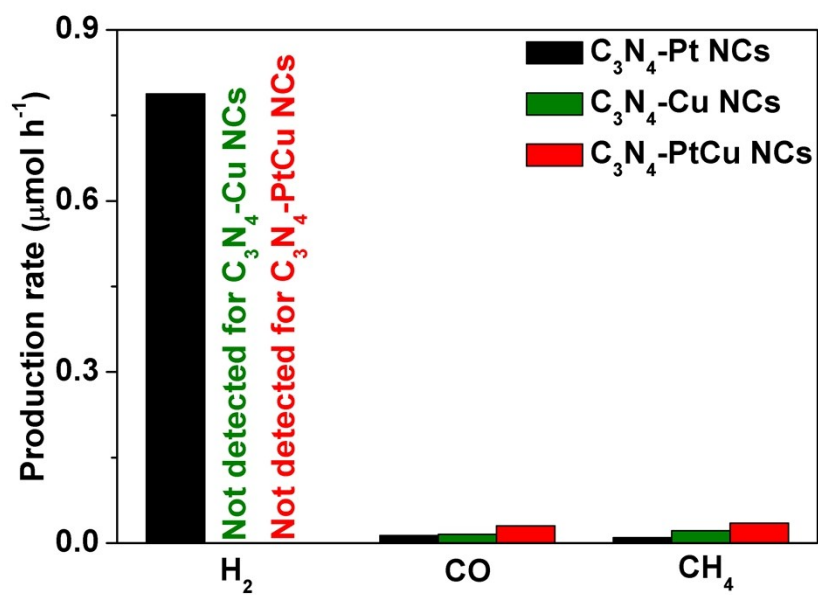
**Fig. S9** Photocatalytic $H_2$, CO, and $CH_4$ evolution rates of $C_3N_4$-Pt NCs and $C_3N_4$-Cu NCs in $CO_2$ reduction reaction with $C_3N_4$-PtCu NCs as a reference sample.

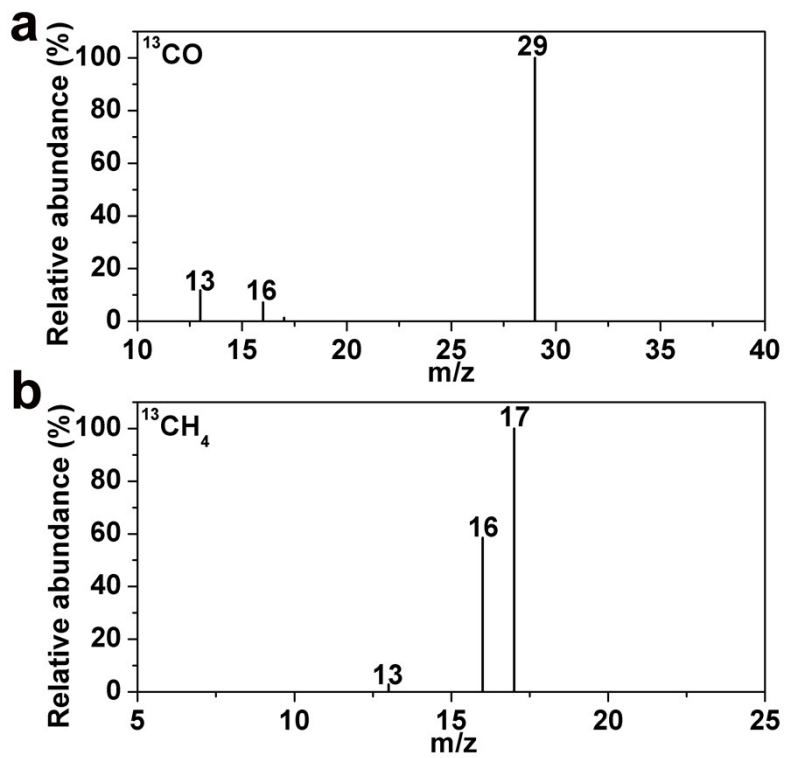**Fig. S10** Results of GC-MS analysis for the (a) $^{13}CO$ and (b) $^{13}CH_4$ produced over $C_3N_4$-PtCu CNCs in photocatalytic reduction of $^{13}CO_2$.
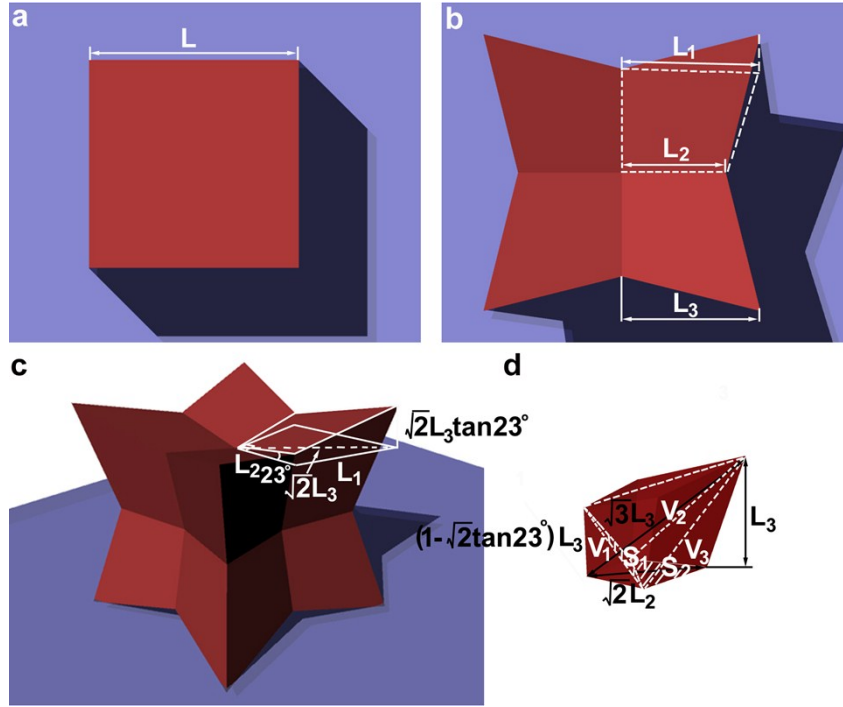
**Fig. S11** Schematic illustration showing the calculation of exposed surface area-to-volume ratio of PtCu nanocubes (S/V$_{\text{PtCu nanocubes}}$) and concave nanocubes (S/V$_{\text{PtCu concave nanocubes}}$) in (a) $C_3N_4$-PtCu NCs and (b-d) $C_3N_4$-PtCu CNCs.

(1) L = 6.1 nm, according to Fig. S10a,

$S_{\text{PtCu nanocubes}} = 5 \times L^2 = 5 \times 6.1 \times 6.1 = 186.5$ nm$^2$

$V_{\text{PtCu nanocubes}} = L^3 = 6.1 \times 6.1 \times 6.1 = 227.0$ nm$^3$

$S/V_{\text{PtCu nanocubes}} = 186.5/227.0 = 0.82$ nm$^{-1}$

(2) $L_1 = 5.2$ nm, $L_2 = 3.8$ nm, according to Fig. S10b-d,

$S_{\text{PtCu concave nanocubes}} = 20 \times (1/2L_2^2 + 1/2 \times \sqrt{L_1^2 - 1/2L_2^2} \times \sqrt{2}L_2) / \cos 23^\circ$

$= 20 \times (0.5 \times 3.8 \times 3.8 + 0.5 \times 4.45 \times 5.37)/0.92 = 416$ nm$^2$

$L_3 = (\sqrt{2}/2L_2 + \sqrt{L_1^2 - 1/2L_2^2}) / \sqrt{2} = 5.0$ nm

$V_{\text{PtCu concave nanocubes}} = 8 \times (V_1 + V_2 + 3V_3)$

$V_1 + V_2 = 1/3 \times S_1 \times \sqrt{3}L_3 = 1/3 \times 8.32 \times 8.66 = 24$ nm$^3$

$V_3 = 1/3 \times S_2 \times L_3 = 1/3 \times 6.97 \times 5 = 11.62$ nm$^3$

$V_{\text{PtCu concave nanocubes}} = 8 \times (24 + 11.62 \times 3) = 470.9$ nm$^3$

$S/V_{\text{PtCu concave nanocubes}} = 416/470.9 = 0.88$ nm$^{-1}$

With the same loading amount of PtCu in $C_3N_4$-PtCu NCs and $C_3N_4$-PtCu CNCs (Table S1), the S/V$_{\text{PtCu nanocubes}}$ (0.82 nm$^{-1}$) and S/V$_{\text{PtCu concave nanocubes}}$ (0.88 nm$^{-1}$) is much similar, confirming the approximate exposed area of PtCu nanocubes and concave nanocubes in $C_3N_4$-PtCu NCs and $C_3N_4$-PtCu CNCs.
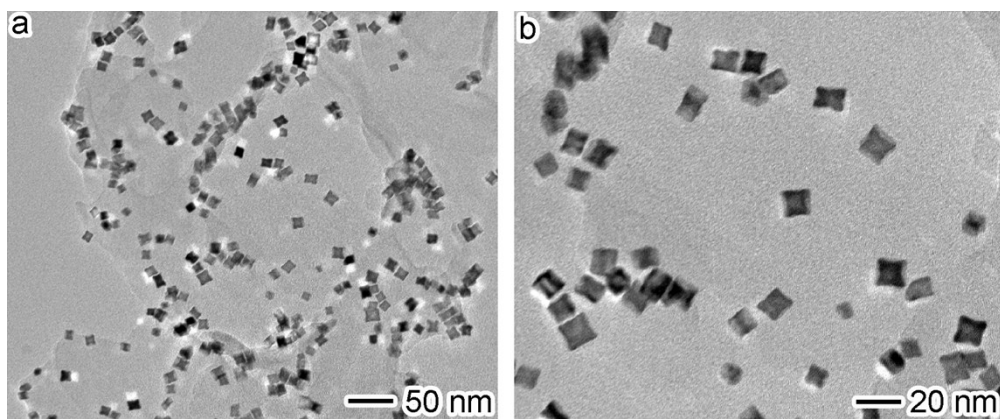
**Fig. S12** TEM images of C$_3$N$_4$-PtCu CNCs after the photocatalytic reaction.
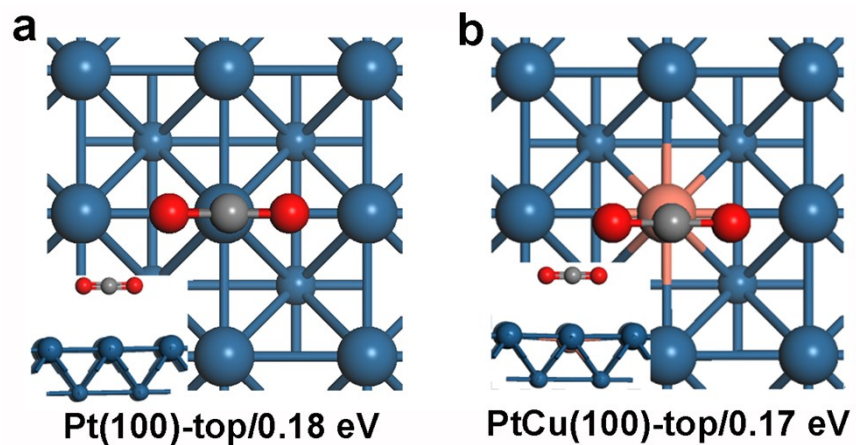
**Fig. S13** Other configurations of $CO_2$ adsorbed on Pt(100) and PtCu(100) facets together with the adsorption energy (dark blue ball for Pt atom; brown, dark and red ones for Cu, C and O atoms, respectively).

**Fig. S14** Other configurations of $CO_2$ adsorbed on Pt(730) facet together with the adsorption energy (dark blue ball for Pt atom; dark and red ones for C and O atoms, respectively).

**a** PtCu(730)-bridge1/-0.40 eV

**b** PtCu(730)-bridge2/-0.28 eV

**c** PtCu(730)-top1/-0.01 eV

**d** PtCu(730)-top2/-0.05 eV

**Fig. S15** Other configurations of $CO_2$ adsorbed on PtCu(730) facet together with the adsorption energy (dark blue ball for Pt atom; brown, dark and red ones for Cu, C and O atoms, respectively).
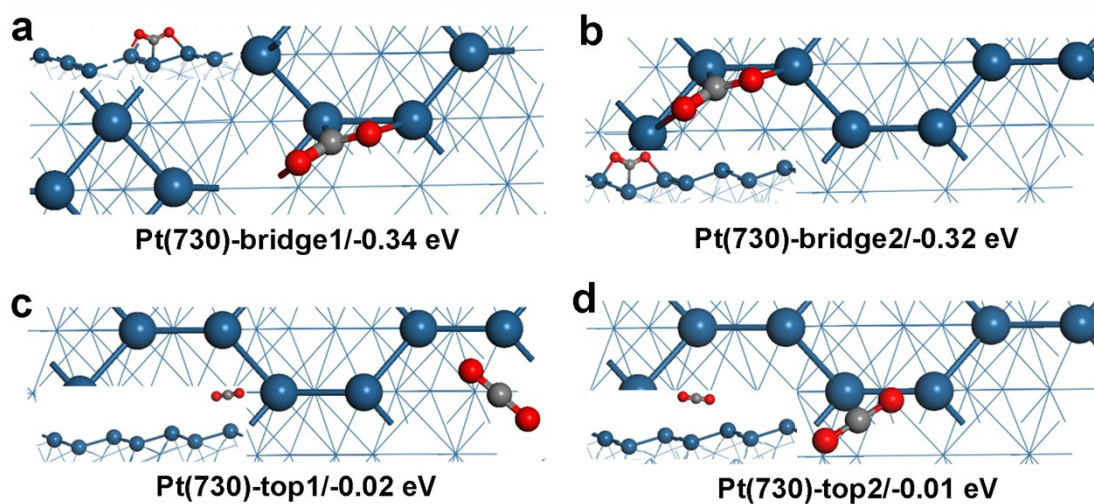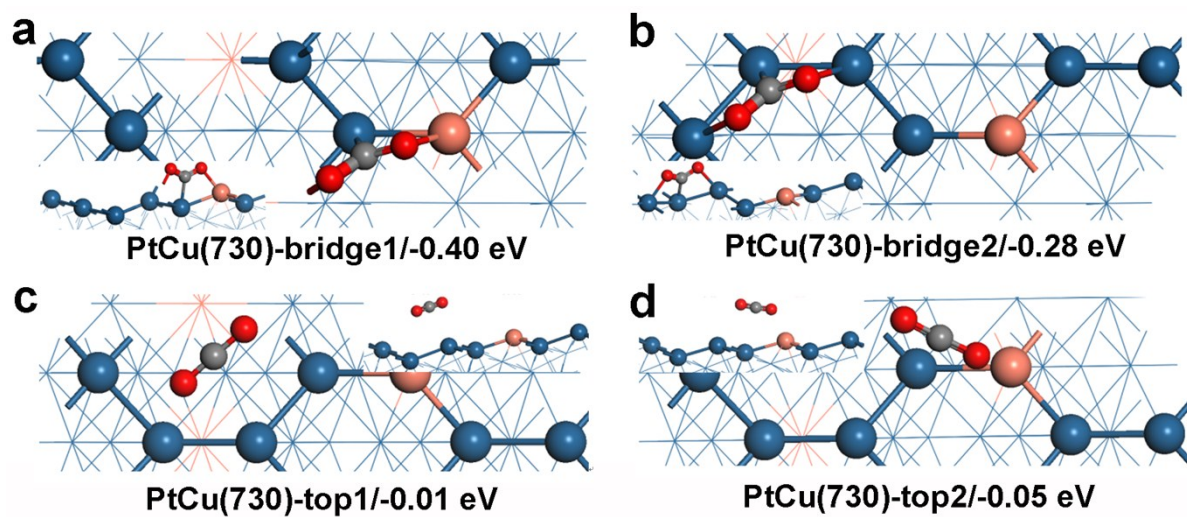
**Table S1** Chemical compositions of the $C_3N_4$-PtCu NCs, $C_3N_4$-PtCu CNCs, $C_3N_4$-Pt NCs and $C_3N_4$-Cu NCs samples determined by ICP-MS.

| Sample | Molar ratio of Pt : Cu | Weight ratio of PtCu : $C_3N_4$ |
|---|---|---|
| $C_3N_4$-PtCu NCs | 87.4 : 12.6 | 9.2 : 100 |
| $C_3N_4$-PtCu CNCs | 86.8 : 13.2 | 9.1 : 100 |
| $C_3N_4$-Pt NCs | 100 : 0 | 9.5 : 100 |
| $C_3N_4$-Cu NCs | 0 : 100 | 9.0 : 100 |

**Table S2** Comparison of the photocatalytic performance of the as-synthesized $C_3N_4$-PtCu CNCs with previously reported $C_3N_4$ supported metal cocatalyst nanostructures without high-index facet.

| Semiconductor | Cocatalyst | Average $CH_4$ production rate per gram of photocatalysts ($\mu$mol $g_{cat}^{-1}$ $h^{-1}$) | Selectivity for $CH_4$ production (%) | Ref. |
|---|---|---|---|---|
| $C_3N_4$ | Pd nanotetrahedrons | 0.3 | 2.5 | 9 |
| $C_3N_4$ | Pd nanoparticles | 0.1 | 3.4 | 62 |
| $C_3N_4$ | Pt nanoparticles | 1.3 | — | 63 |
| $C_3N_4$ | Pt nanoparticles | 0.3 | 57.1 | 64 |
| $C_3N_4$ | PtCu concave nanocubes | 7.5 | 90.6 | a |

[a] The photocatalytic performance of $C_3N_4$-PtCu CNCs reported by us.

**Table S3** Mulliken charges of C, O and $CO_2$ on Pt and PtCu models.

| Configurations | Mulliken charge | | | |
|:---:|:---:|:---:|:---:|:---:|
| | O | C | O | $CO_2$ |
| Pt(100)-bridge | -0.420 | 0.800 | -0.420 | -0.04 |
| PtCu(100)-bridge | -0.420 | 0.800 | -0.430 | -0.05 |
| Pt(730)-bridge | -0.430 | 0.370 | -0.430 | -0.49 |
| PtCu(730)-bridge | -0.450 | 0.360 | -0.450 | -0.54 |

**References**

S1 H. Guo, Y. Chen, M. B. Cortie, X. Liu, Q. Xie, X. Wang and D. L. Peng, *J. Phys. Chem. C*, 2014, **118**, 9801.